MEACS2015 **IOP Publishing** 

IOP Conf. Series: Materials Science and Engineering 124 (2016) 012018 doi:10.1088/1757-899X/124/1/012018

# Application of mathematical modelling methods for acoustic images reconstruction

## I Bolotina, A Kazazaeva, K Kvasnikov and A Kazazaev

Tomsk Polytechnic University, 30, Lenina ave., Tomsk, 634050, Russia

E-mail: bolotina@tpu.ru

Abstract. The article considers the reconstruction of images by Synthetic Aperture Focusing Technique (SAFT). The work compares additive and multiplicative methods for processing signals received from antenna array. We have proven that the multiplicative method gives a better resolution. The study includes the estimation of beam trajectories for antenna arrays using analytical and numerical methods. We have shown that the analytical estimation method allows decreasing the image reconstruction time in case of linear antenna array implementation.

## 1. Introduction

Currently, ultrasonic non-destructive testing is facing an increasingly relevant problem of considerable improvement of spatial resolution and bringing the dimensions of inspected region closer to the length of probing signal ultrasonic wave  $\lambda$ . This problem can be solved by focusing ultrasonic radiation in the selected point of space. If the inspection depth and ultrasonic transducer dimensions are comparable with wavelength  $\lambda$ , the focusing is practicable only with the use of synthesized aperture having quite large dimensions as compared to the wavelength. Synthetic Aperture Focusing Technique (SAFT) becomes increasingly popular for flaw detection in fine structure materials and medical diagnostics, where it is used for the sake of improved resolution and image quality [1, 2].

SAFT is based on irradiating of a selected point of the inspected region from different directions from the inspection surface, receiving echo-signals from this point also from different directions, and summing the received signals with preliminary addition of time delays to them. This will compensate the differences in distances (time of signal travel) from surface points to the selected point of the inspected semi-space. The generation of a two-dimensional image (tomogram) of the section of the inspected object requires repeating the described procedure for each point of the selected crosssection.

## 2. Image Reconstruction Using SAFT

Synthetic Aperture Focusing Technique (SAFT) provides for a high rate of the image reconstruction, testing accuracy and an improved signal-to-noise ratio as compared to a conventional phased array.

One of the most significant advantages of SAFT is the capability of increasing a signal-to-noise ratio. Numerous sources of noise determined individually usually form a noise that is characterized by probabilistic parameters. A SAFT processing algorithm implies coherent summation of signals of individual elements comprising the antenna array. In case of normal law of noise probability density IOP Conf. Series: Materials Science and Engineering 124 (2016) 012018 doi:10.1088/1757-899X/124/1/012018

distribution, the increase of the signal-to-noise ratio is proportional to the number of elements in the array.

The other benefit of phased antenna arrays is the capability of generating two-dimensional and three-dimensional images of defects. This feature is due to the capability of scanning by controlling an antenna pattern within the required inspection zone. In all probability, the inspection zone can be considered as a linear field; hence, it has the property of additivity. The obtained data comprise a discrete set, which characterizes the state of each separate point of the scanning region. In the method of echo sounding, the regularity of a formed response signal will be primarily based on such characteristic as an antenna pattern. The SAFT-algorithm suggests the realization of the integral value of this parameter in both radiation and reception modes.

Implementation of SAFT is based on computational processing of a large amount of data. All equations describing this method include the embedded summation. In this connection, the application of such equations without computers is practically impossible.

## 3. Additive and Multiplicative Method for Processing Signals from Antenna Array

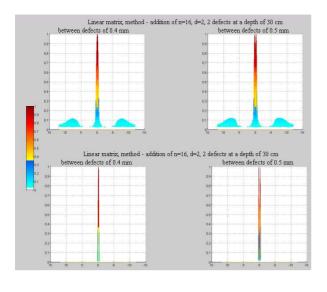
SAFT has a large number of modifications that are determined by the method of signal processing. There are such methods as SAFT-C, M-C-SAFT, TS-M-C-SAFT, SPA (Sampling Phased Array) [3, 4], etc.

To estimate acoustic fields, this work has used a multiplication method instead of SPA summation used in the original method. The use of the multiplicative method has the following advantages:

- improved signal-to-noise ratio;
- decreased sidelobe level of the antenna pattern.

The following drawbacks can be mentioned: increased computation time (multiplication is more complex for computers as compared to summation); the necessity of normalized signal received from the transducer stipulated by an overflow caused by multiple multiplications.

Figure 1 demonstrates the antenna patterns of linear antenna arrays received using additive and multiplicative methods of signal treatment. Figure 1 shows that the use of the multiplicative method of signal processing provides a considerably better resolution, while the sidelobe level is lower than that in case of the additive signal processing method.



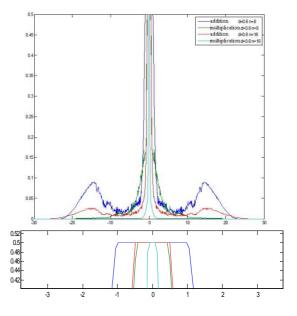


**Figure 1.** Antenna patterns of linear antenna arrays received using additive and multiplicative methods of signal treatment

IOP Conf. Series: Materials Science and Engineering 124 (2016) 012018 doi:10.1088/1757-899X/124/1/012018

## 4. Real-time Signature Formation

A real-time image reconstruction requires achieving the time of single image generation of at least 1/24 of a second. During the image reconstruction using SAFT, one of the most complex tasks from computational point of view is determination of a trajectory of ultrasound passing from the piezoelectric transducer to the selected inspection point. The necessity of this process is imposed by breaking the inspected object into local regions and considering each local region as a point-like reflecting element. Echo-signals received by each piezo-transducer of the antenna array are shifted back temporarily for the value, which is equal to the time of wave propagation reflected from the inspected local region to a corresponding antenna array piezo-transducer. Then, the time-shifted signals of all antenna array piezo-transducers are summed respectively for each inspected region. The acquired signal amplitude for each local region is mapped by colour and displayed on a monitor [5, 6].

Let us determine the beam trajectory for linear antenna array. It is well known that in the case of the immediate contact of the multi-element antenna array with an inspected object, the width of the intermediate layer of immersion liquid can be neglected (Figure. 2). Then, the calculation of distances from transmitter (point D) to given inspection point (point P) is trivial and comes to the solution of the following quadric equation (1)

$$l_{\rm D-P} = \sqrt{(x_0 - x_d)^2 + y_0^2}$$
 (1)

where  $x_0, y_0$  are coordinates of inspection point P;  $x_d$  is the distance from the centre of antenna array to a transducer.

In case when an intermediate agent, for instance, water or a prism, is between the antenna array and the material under inspection, the estimation of paths of ultrasonic waves becomes slightly more complex (Figure. 3).

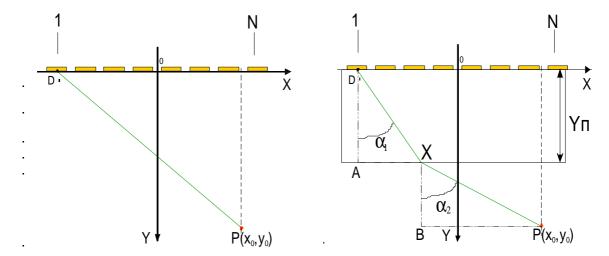


**Figure 2.** Scheme of ultrasound transmission from the linear antenna array in case of the contact inspection method

**Figure 3.** Scheme of ultrasound transmission from the linear antenna array in case of inspection through a prism

Snell's law describes a process of transmission and refraction of waves through an interface by the following equation (2)

$$c_2 \cdot \sin \alpha_1 = c_1 \cdot \sin \alpha_2,\tag{2}$$

where  $c_1$  is sound velocity in the first medium (a prism);  $c_2$  is sound velocity in the second medium (inspection object);  $\alpha_1$  is a wave incidence angle in the first medium (a prism);  $\alpha_2$  is an angle of refracted sound in the second medium (an inspection object);

IOP Conf. Series: Materials Science and Engineering 124 (2016) 012018 doi:10.1088/1757-899X/124/1/012018

in order to find point X, we shall express  $sin(\alpha_1)$  as a ratio of side AX to hypotenuse DX, and  $sin(\alpha_2)$  as a ratio of side BP to hypotenuse PX (Figure. 3). Then we shall insert the obtained values into Snell's law and take the square of the right and left parts. In this case,

$$c_2^2 \cdot \frac{(x - x_d)^2}{(x - x_d)^2 + y_n^2} = c_1^2 \cdot \frac{(x_0 - x)^2}{(x_0 - x)^2 + (y_0 - y_n)^2},$$
(3)

where  $y_n$  is the height of the prism (an intermediate layer); x is the point of refraction at interface, where angles  $\alpha_1$  and  $\alpha_2$  (Figure.3) shall provide for the compliance with Snell's law.

Having reduced expression (3) to a common denominator and having grouped the coefficients by exponent x, we come to the following expression in the numerator:

$$x^4 \cdot (c_2^2 - c_1^2) +$$

$$\begin{aligned} &2\cdot x^3\cdot (-c_2^2\cdot x_0-c_2^2\cdot x_d+c_1^2\cdot x_0+c_1^2\cdot x_d) + \\ &x^2\cdot (c_2^2\cdot x_0^2+c_2^2\cdot (y_0-y_n)^2+c_2^2\cdot 4x_d\cdot x_0+c_2^2\cdot x_d^2-c_1^2\cdot x_0^2-c_1^2\cdot x_d^2-c_1^2\cdot y_n^2-c_1^2\cdot 4x_0\cdot x_d) + \\ &x\cdot (-c_2^2\cdot 2x_d\cdot x_0^2-c_2^2\cdot 2x_d\cdot (y_0-y_n)^2-c_2^2\cdot 2x_d^2\cdot x_0+c_1^2\cdot 2x_0^2\cdot x_d+c_1^2\cdot 2x_0\cdot x_d^2+c_1^2\cdot 2x_0\cdot y_n^2) + \end{aligned}$$

$$c_2^2 \cdot x_d^2 \cdot x_0^2 + c_2^2 \cdot x_d^2 \cdot (y_0 - y_n)^2 - c_1^2 \cdot x_0^2 \cdot y_n^2 - c_1^2 \cdot x_0^2 \cdot x_d^2 = 0$$

Later on, to simplify the expression let us denote the coefficients of the derived equation, such as a, b, c, d, e.

Taking into account the non-zero denominator, we obtain  $(x-x_d)^2+y_n^2\neq 0$  and  $(x_0-x_0)^2+(y_0-y_n)^2\neq 0$ 

If we adopt

$$p = \frac{8ac - 3b^2}{8a^2}; q = \frac{8a^2d + b^3 - 4abc}{8a^3}; r = \frac{b^2c}{16a^3} - \frac{bd}{4a^2} - \frac{3b^4}{256a^4} + \frac{e}{a},$$
 (5)

then after solving the acquired quartic equation through Ferrari's solution [7], we get the following roots:

$$x_{1,2,3,4} = \frac{\pm\sqrt{2z_1} \pm\sqrt{2z_1 - 4\left(\frac{p}{2} + z_1 + \frac{q}{2\sqrt{2z_1}}\right)}}{2} - \frac{b}{4a},\tag{6}$$

where  $z_1$  is the first real root of the equation.

$$z^{3} + pz^{2} + \frac{p^{2} - 4r}{4}z - \frac{q^{2}}{8} = 0.$$

The roots of equations (6) are fairly complex to find. In this connection, one can assume that the numerical method will happen to be less time-consuming. To check this assumption, we will formulate the numerator from equation (3) as

$$f1(x) = c_2^2 \cdot (x - x_d)^2 \cdot ((x_0 - x_0)^2 + (y_0 - y_n)^2) - c_1^2 \cdot (x_0 - x_0)^2 ((x - x_d)^2 + y_n^2)$$
(7)

and find the value of x using the numerical method that will correspond to the value of function fI being less than 0.1 of the physical dimensions of the inspection point.

If sound velocity in the prism is less than that in the inspected material, then angle  $\alpha_2$  will be larger than angle  $\alpha_1$ . Hence, desired point X will be between  $x_d$  and  $x_0$ . Let us take these points as starting ones so that we can search and find the solution through chord method [7].

MEACS2015 IOP Publishing

IOP Conf. Series: Materials Science and Engineering 124 (2016) 012018 doi:10.1088/1757-899X/124/1/012018

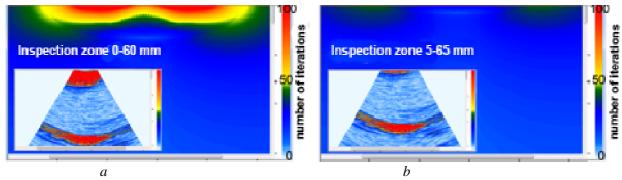


**Figure. 4.** Distribution of the number of iterations for different inspection zones. a) is an inspection zone from 0 to 60 mm; b) is an inspection zone from 5 to 65 mm.

Figure 4a depicts the distribution of the number of iterations necessary for estimating distances from a transducer to the selected point of the inspection zone. The number of iterations is colour-mapped; the principle of colour-mapping is described in the right Figure as a histogram. The insert in Figure 4a shows that the reconstruction of the inspection zone is performed on the basis of estimated distances.

We have experimentally established that the largest number of iterations (red zone, more than 100 iterations per point) corresponds to the interfaces. So-called 'dead zone' is also located there. For instance, if we shift the inspection zone by five millimetres into the material, the points with the largest number of iterations will almost disappear (Figure. 4b). Moreover, the 'dead zone' is almost completely cut off (an insert in Figure. 4b) and the total number of iterations decreases, which leads to shortened estimation time.

#### 5. Conclusions

The use of the multiplicative method of signal processing provides for a considerably better resolution of SAFT, while the side lobe level on the antenna pattern is lower than that in case of the additive signal processing method.

The use of the analytical estimation method allows decreasing the image reconstruction time in case of linear antenna array implementation. The estimation time increases proportionally to the number of displayed points. In case of a large number of displayed points, the real-time image reconstruction is impossible. One of the possible solutions of this problem is shifting to hardware processing on the basis of FPGA logic, which can be used for the analytical estimation method.

## Acknowledgments

The study was financially supported by the Ministry of Education and Science of the Russian Federation within the Federal Target Program entitled 'R&D in Priority Areas of Development of Russia's Scientific and Technological Complex for 2014–2020' (unique project ID: RFMEFI57514X0048).

## References

- [1] Kozlov V N, Samokrutov A A, Yakovlev N N, Kovalev A V and Shevaldykin V G 1989 Control equipment and systems 7 21-23
- [2] Thomson R H 1983 *Ultrasonics* **21** 11-18
- [3] Badalian V G, Bazulin E G and Vopilkin A Kh 2009 Moscow: Mashinostroeniye
- [4] Bulavinov A, Kröning M, Pinchuk R and Reddy K M 2009 Münster: Jahrestagung
- [5] Soldatov A I, Seleznev A I, Soldatov A A, Sorokin P V and Makarov V S 2012 Russian Journal of Nondestructive Testing 48 268-271

[6] Bolotina I O, Kroening H-M, Kvasnikov K G, Sednev D A and Sumtsova O V 2014 *Advanced Materials Research* **1040** 959-964

[7] Korn G and Korn T 2003 Nauka: Moscow